The model SIRANE for atmospheric urban pollutant dispersion. PART III: Validation against NO$_2$ yearly concentration measurements in a large urban agglomeration

L. Soulhac, C.V. Nguyen, P. Volta, P. Salizzoni[*]

Laboratoire de Mécanique des Fluides et d'Acoustique, UMR CNRS 5509 University of Lyon, Ecole Centrale de Lyon, INSA Lyon, Université Claude Bernard Lyon I, 36, Avenue Guy de Collongue, 69134 Ecully, France

HIGHLIGHTS

- We present a validation study of an updated version of the SIRANE model.
- Model results are compared to field data collected in Lyon over a whole year.
- SIRANE reproduces well spatial and temporal variations of pollutant concentrations.
- Analysis of the results allows identifying possible improvements of the model.

GRAPHICAL ABSTRACT
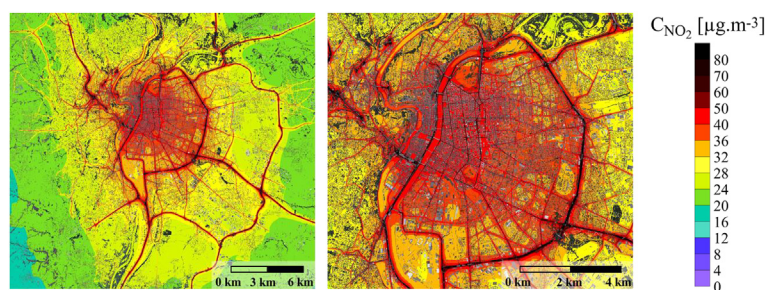
ABSTRACT

We present a validation study of an updated version of the SIRANE model, whose results have been systematically compared to concentrations of nitrogen dioxide collected over the whole urban agglomeration of Lyon. We model atmospheric dispersion of nitrogen oxides emitted by road traffic, industries and domestic heating. The meteorological wind field is computed by a pre-processor using data collected at a ground level monitoring station. Model results are compared with hourly concentrations measured at 15 monitoring stations over the whole year (2008). Further 75 passive diffusion samplers were used during 3 periods of 2 weeks to get a detailed spatial distribution over the west part of the city. An analysis of the model results depending on the variability of the meteorological input allows us to identify the causes for peculiar bad performances of the model and to identify possible improvements of the parameterisations implemented in it.

© 2017 Elsevier Ltd. All rights reserved.

1. Introduction

Nowadays, there are four different main approaches generally adopted for the operational modelling of the atmospheric pollutant dispersion at the urban scale: i) modified Gaussian models (e.g. Stocker et al., 2012), Lagrangian models (e.g. Tinarelli et al., 2012), fast Computational fluid Dynamics models (e.g. Brown et al., 2013), and street network models (e.g. Soulhac et al., 2011). Despite an increasing interest in the street network approach arising in recent years (Belcher et al., 2015), it remains the less employed, and as far as we are aware, SIRANE (Soulhac et al., 2012, 2011) is the only operational model based on this approach which is currently used for air quality evaluations. In France, SIRANE is adopted by several

* Corresponding author.
   E-mail address: pietro.salizzoni@ec-lyon.fr (P. Salizzoni).

local authorities for air pollution management and is used for the pollutant exposure assessment in epidemiologic studies (Jacquemin et al., 2013; Morelli et al., 2016; Ouidir et al., 2015; Padilla et al., 2016). Other pilot studies on urban air pollution have been performed in Turin (Castagnetti et al., 2008; Garbero et al., 2010), Florence (Giambini et al., 2010), and Milan (Biemmi et al., 2010).

To date, the SIRANE model has been validated against both wind tunnel experiments (Carpentieri et al., 2012; Salem et al., 2015; Soulhac, 2000) and on-site measurements. However, the only validation study published in the literature and based on open field measurements is limited to a unique district of Lyon and over a time period of two weeks only (Soulhac et al., 2012). This paper aims in filling this gap, by presenting an exhaustive validation of the SIR-ANE model at the urban scale based on on-site measurements, similar to those realised for other similar models, e.g. ADMS-Urban (Dėdelė and Miškinytė, 2015; Harsham and Bennett, 2008; Mohan, 2011; Righi et al., 2009).

This new validation study, which is intended to complete previous results presented by Soulhac et al. (2012), is performed over a whole year (2008) and over the whole urban area of Lyon (36 × 40 km) with an updated version of the model (SIRANE 2.0).

2. Description of the SIRANE 2.0 model

SIRANE is an operational model simulating pollutants dispersion at the local urban scale, assuming steady meteorological conditions over hourly time steps (Soulhac et al., 2011). The inputs of the SIRANE model are the urban geometry, the meteorological data, the industrial, traffic, and surface emissions, and the background concentration. The only chemical reactions taken into account concern the Chapman cycle $NO-NO_2-O_3$, computed assuming a photo-stationary equilibrium (Seinfeld, 1986).

In the urban canopy, the street network is represented by a series of connected boxes, each of them characterised by a length L, width W, height H, and having walls characterised by a uniform aerodynamic roughness. The pollutant concentration in each street is estimated by means of a mass balance taking into account three main transfer processes: the convective transport along the street, the turbulent transfer at roof level, and the dispersion at street intersections.

The atmospheric flow above roof level is modelled as a surface boundary layer over a rough surface and pollutant dispersion is modelled by means of a generalised Gaussian puff model, with ground reflection. Standard deviations of the Gaussian puffs are computed according to the Monin-Obukhov similarity theory. Note that, in the previous version of the SIRANE model, the dispersion patterns occurring over subsequent hourly time steps were considered as independent one from the other. This is a main limitation when simulating dispersion under low-wind conditions, during which the pollutant emitted within the domain are not necessarily advected outside of it within an hour. To overcome this limitation, SIRANE 2.0 adopts a Gaussian puff model, based on a double error function distribution (Cierco et al., 2010), and aggregating emissions occurring over previous time steps within large grid cells (typically 1 km × 1 km). The emissions include elevated sources (industries) and surface distributed sources (domestic heating) as well as all contributions given by the vertical fluxes at roof level, due to the turbulent exchanges between street canyons and overlying atmosphere (modelled as series of point sources at roof height). Note that, in an urban area of a medium European city, the street network can be made up of several tens of thousands of streets, so that the calculation of pollutants concentration in the overlying atmosphere requires summing the contribution of tens of thousands Gaussian plumes. From a computational point of view,

this task is therefore very expensive when considering a large number of receptors. In the case considered in this paper for example, the concentration map of consists in a 10 meters resolution grid on a 36 km × 40 km domain, i.e. 14.4 millions of receptors (see graphical abstract). To reduce this computational time, SIRANE 2.0 adopts a new algorithm. This allow evaluating the pollutant concertation at a given receptor, by differentiating the contribution of sources placed close to it, within a given buffer zone, and all other sources located outside of it. Within the near-field buffer region all pollutant emissions at roof level and above it are treated individually and modelled by a Gaussian puffs. All other sources located outside this buffer, whose dimensions are of order 1.5 × 1.5 km, are instead aggregated into surface sources of dimensions 300 m × 300 m.

3. Case study

The study concerns the urban Agglomeration of Lyon over a 36 km × 40 km domain. Time-series of NO_2 concentration used for the model validation were collected in different measurement sites (Fig. 1) over the whole year 2008 by Atmo Auvergne Rhone Alpes, the local authority for air quality. These include hourly measurements provided by 15 permanent measurement stations, which can be classified in 4 different categories: suburban stations (Côtière de l'Ain, Genas, Saint-Exupéry et Ternay), stations placed on high-intensity traffic roads (Berthelot, Grand-Clément, Lyon périphérique, Mulatière et Vaise), stations close to industrial sites (Feyzin et Saint-Fons) and stations within the urban agglomeration and away from high-intensity traffic roads (Gerland, Lyon centre, Saint-Just et Vaulx-en-Velin). For these stations, missing hourly data do not exceed 3% over the whole year 2008. The validation is based on the concentration of NO_2 for two main reasons: i) NO_X emissions estimates are generally more reliable than those of PM (Pouliot et al., 2015); ii) estimating NO_2 concentration requires a chemical module to simulate the Chapman cycle.

Since almost no data was available for the west part of the city, measurements from these 15 stations were completed with series of two-week average measurements by means of passive diffusion tubes (PDT) located over 75 sites (Fig. 1) during Intensive Observational Periods (IOP).

The three IOPs of two weeks each (Table 1) allowed us to have measurements in different periods of the year and namely in winter, in summer and in an intermediate season (spring). The duration of each period was limited by the availability of our economic resources. All 3 IOPs for the PDTs use the same sampling sites. Each IOP is broken out into two one-week periods, since during each IOP we performed two independent measurements of one week each. The location of the PDTs was chosen in order to cover a part of the town which is densely populated and where there are no fixed monitoring stations. Their location was also chosen in order to cover different kind of land use and in order to have a high spatial resolution of the concentration field, at least in this limited part of the domain.

It is well known (e.g. Nash and Leith, 2010) that PDTs generally tend to overestimate pollutant concentrations. This feature was also extensively discussed in the Part II of the present study (i.e, Soulhac et al., 2012), where we also provided a detailed digression of the experimental methods for using the PDTs and their characteristics (precision and accuracy). Therefore, during the intensive observation periods, we have placed 3 temporary stations equipped with analysers in the same positions of three passive diffusion tubes: Valvert, Francheville and Pierre Benite. The positions of these three movable stations are shown in Fig. 1. The comparison between the two sets of data allowed us to find a calibration coefficient of the PDTs (see Fig. 2).
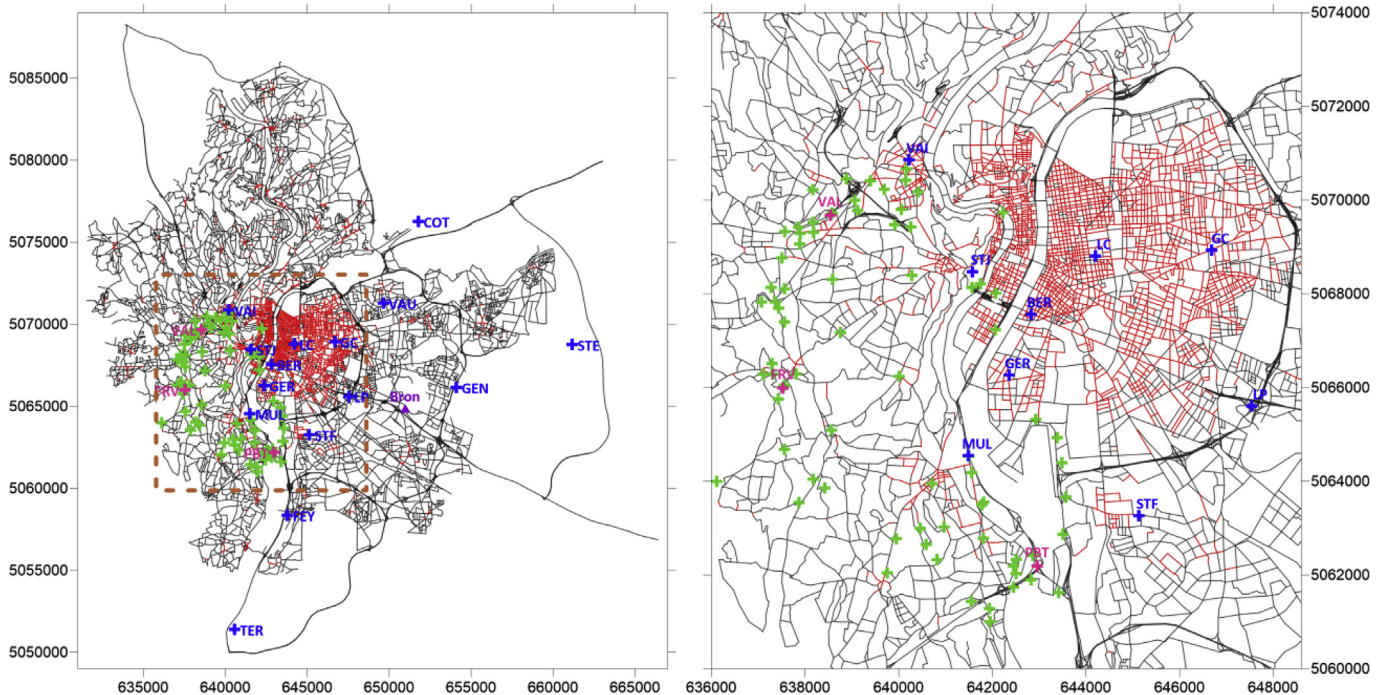
Fig. 1. Studied domain and network of streets of the SIRANE simulation (UTM31 coordinates). Street canyons are represented in red and open roads are represented in grey. Monitoring stations are represented in blue (BER: Berthelot; COT: Côtière de l'Ain; FEY: Feyzin; GC: Grand-Clément; GEN: Genas; GER: Gerland; LC: Lyon centre; LP: Lyon périphérique; MUL: Mulatière; STE: Saint-Exupéry; STF: Saint-Fons; STJ: Saint-Just; TER: Ternay; VAI: Vaise; VAU: Vaulx-en-Velin). Passive samplers are represented in green. Bron meteorological station is in violete. The three movable stations for the IOPs are in rose: VAI: Vaise; FRV: Francheville; PBT: Pierre Benite. (For interpretation of the references to colour in this figure legend, the reader is referred to the web version of this article.)

Table 1
Dates of the intensive observational periods.

| IOP	Begining of exposure	End of exposure
IOP 1 − Week 1	30/01/2008 13 h	06/02/2008 13 h
IOP 1 − Week 2	06/02/2008 13 h	13/02/2008 13 h
IOP 2 − Week 1	30/04/2008 12 h	07/05/2008 14 h
IOP 2 − Week 2	07/05/2008 14 h	14/05/2008 13 h
IOP 3 − Week 1	16/07/2008 13 h	23/07/2008 13 h
IOP 3 − Week 2	23/07/2008 13 h	30/07/2008 13 h
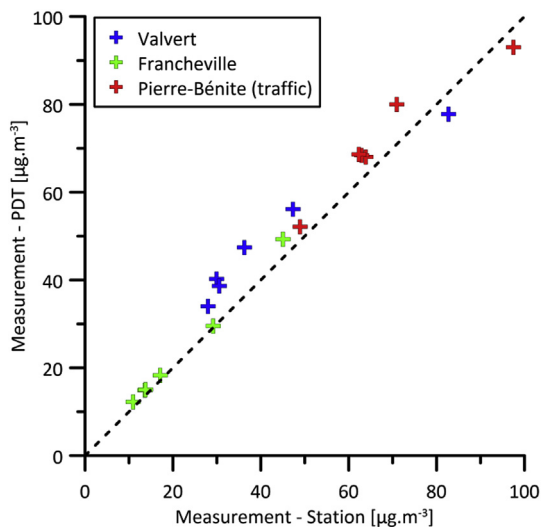
Fig. 2. Calibration of the PDTs measurements against measurements provided by analyzers placed on movable monitoring stations.

The domain includes a network of 21833 streets (Fig. 1), whose geometrical characteristics have been determined using the numerical tools presented in Soulhac et al. (2011), and applied to a GIS data set. This allows us to compute for each street, its length L, height H and width W, and to identify the streets that are classified as 'canyons', i.e. with an aspect ratio W/H $\leq$ 3. These cover approximately 15% of the total length of the street network. The geometrical characteristics of the street canyons within the domain are given in Fig. 3, where we show the probability density functions of the aspect ratios L/H and W/H of all street labelled as 'canyons'.

The preparation of the input of the traffic related emissions is the same as that presented in Soulhac et al. (2012). Traffic emissions are represented as line sources whose intensity is estimated by coupling the traffic model DAVISUM with the emission model COPERT IV (Ntziachristos and Samaras, 2000).

In the domain, we also consider 83 elevated sources (industries) and distributed emissions from domestic heating and other sources, provided by the emission cadaster of the air-quality association of the Auvergne Rhône Alpes region. The cadaster is built with a top/down (dis-aggregation of national data to city-level data) and a bottom/up approach (aggregation of local data like traffic count to city-scale level data) combined with the use of emissions factors from modelling or metrological experimentations. Sources are classified, based on the activity sectors according to the Selected Nomenclature for Air Pollution (SNAP) and considered as a European standard. The inventory, made at the city-level, was distributed and spatially aggregated on a regular 1 × 1km grid. Each cell contains contributions of the 11 SNAP source categories. The distribution of traffic, industrial and domestic heating sources (as annual average) is plotted in Fig. 4. The emissions of the domestic heating are modulated over the year according to the external air temperature.

The meteorological wind field is reconstructed with an hourly

a)

b)
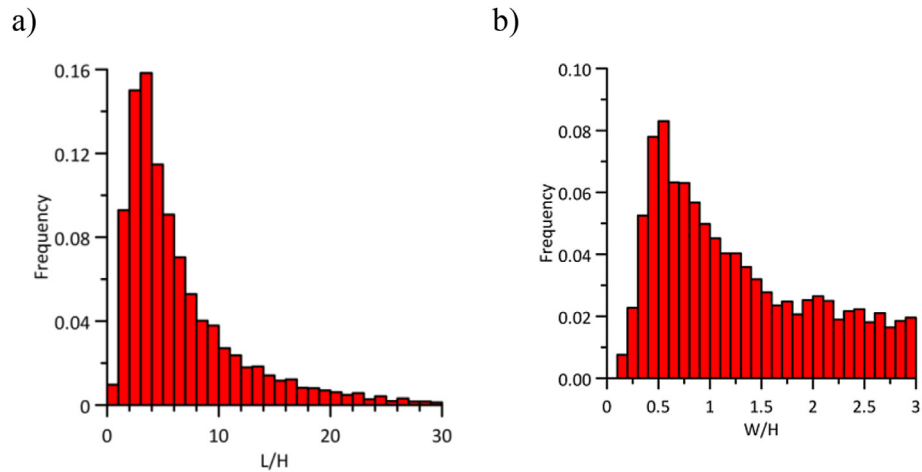
Fig. 3. Geometrical characteristics of the network of street canyons in Lyon: a) histograms of the non-dimensional length L/H of the canyons and of their b) aspect ratio W/H.

a)

b)

c)
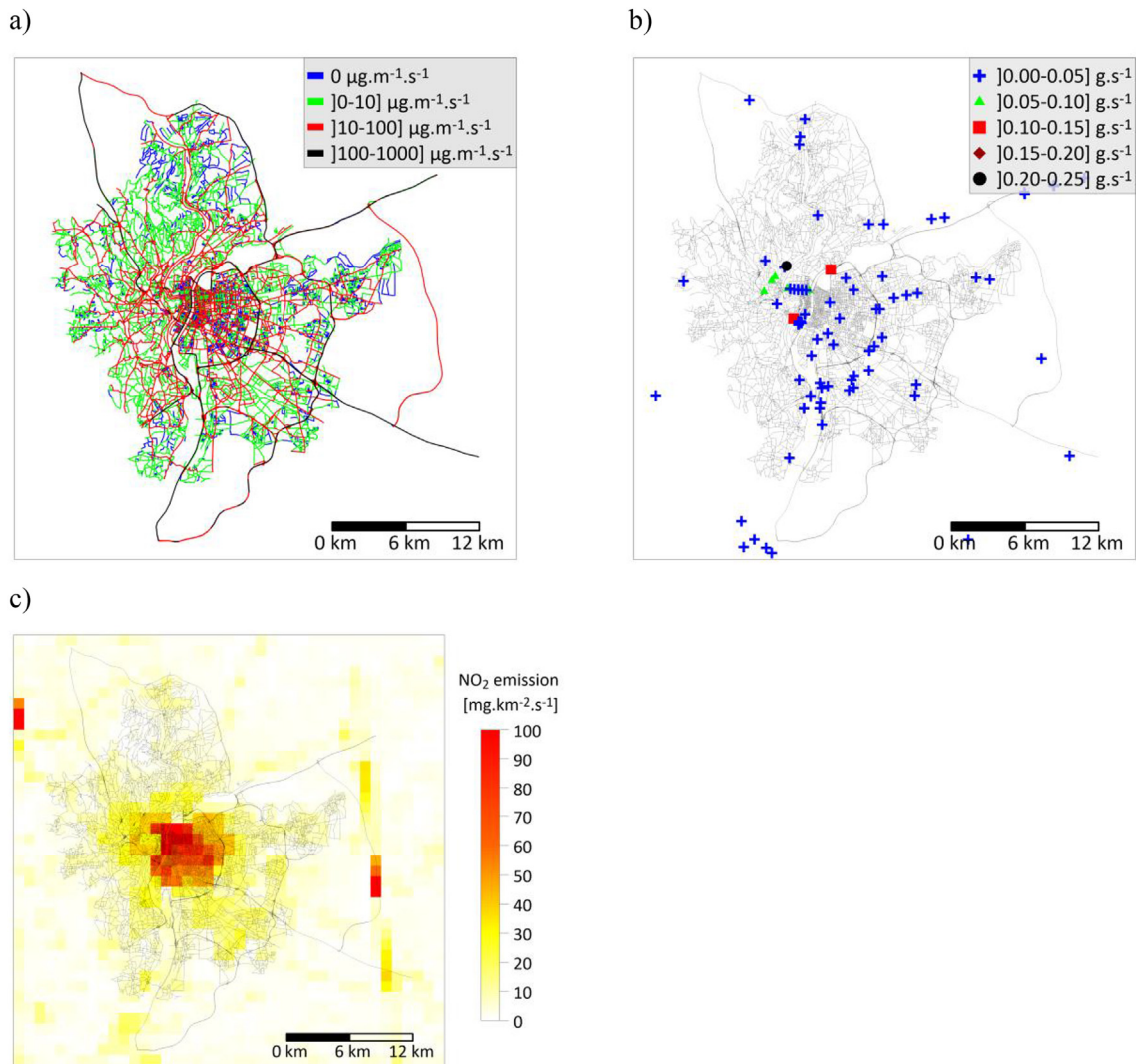
Fig. 4. Spatial distribution of the intensity of the a) traffic (line) sources, b) industrial (point) sources, and c) surface distributed domestic heating sources.

time-step and according to the Monin-Obuhkov similarity theory, from data registered at the Météo-France station in Bron (Fig. 1). Dominant wind direction is North-South, with wind speeds that

generally do not exceed 6 m s^{-1} (Fig. 5a). The stability conditions computed by the meteorological pre-processor are presented in Fig. 5b, where we plot the inverse of the Monin-Obukhov length
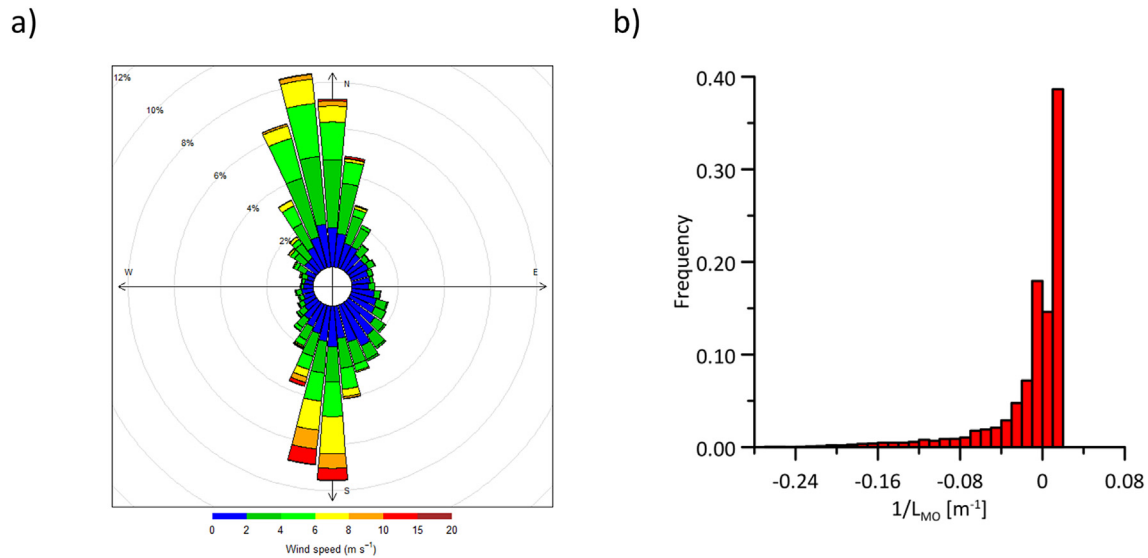
a)

b)

Fig. 5. Annual statistics of data collected at the Bron meteorological station in 2008: a) Windrose and b) probability density function of the ratio $1/L_{MO}$.

(L_{MO}). The distribution of L_{MO}^{-1} suggests an equal repartition between stables ($L_{MO}>0$) and unstable ($L_{MO}<0$) atmospheric conditions. Note that the high frequency of the condition L_{MO}^{-1} in the range $]0.1; 0.2]$ is due to the fact that we have imposed a minimum value for $L_{MO} = 100\ z_0$ (De Haan, 1999), where z_0 is the aerodynamic roughness length of the urban area. The reason for this is to exclude high stability conditions whose occurrence, over an urban area, are precluded by the presence of heat anthropogenic fluxes and intense wind shear.

The estimate of a background concentration is a major problem for the modelling of pollutant concentration at the local urban scale (Tchepel et al., 2010). This concentration is due to the contribution of all pollutant sources located outside the studied domain. These can be estimated by measurements of monitoring stations placed at the border of the domain and far away from traffic axes (Dėdelė and Miškinytè, 2015; Giambini et al., 2010; Tchepel et al., 2010) or by running a dispersion model over a larger (regional) domain (Pineda Rojas and Venegas, 2013; Silver et al., 2013; Soulhac et al., 2003). Here we use as background values the concentration measured at the Saint-Exupéry monitoring station, located at the east border of the domain and at a distance of approximately 30 km from the city center (its location is referred to as 'STE' in Fig. 1). This background concentration is considered as uniformly distributed all over the domain and added to the concentrations estimated by SIRANE before applying the chemistry module.

As it is customary in the recent literature, the performances of the SIRANE model are evaluated by means of statistical indices (Table 2), as proposed by Chang and Hanna (2004). These indices are: the fractional bias FB, the relative error ER, the normal mean square error NMSE, the correlation coefficient Corr, the geometric mean bias MG, the geometric variance VG and the fraction of prediction within a factor of two of observations (FAC2).

Optimal values of these indices, i.e. provided by a perfect model, are 0 for FB, ER and NMSE, and 1 for Corr, MG, VG et FAC2. According to Chang and Hanna (2004) et Chang et al. (2005) the performances of a model can be considered as 'good' if the following criteria are met: $-0.3 \leq$ FB ≤ 0.3, NMSE≤ 4, $0.7 \leq$ MG ≤ 1.3, VG ≤ 1.6 et FAC2 ≥ 0.5. Note that these scores are more restrictive than those presented recently by the same authors for the case of urban areas (Hanna and Chang, 2012). Comparisons with data provided by PDTs are of course averaged over the two

weeks along which the experimental data have been collected.

4. Model performances

As a first step, we analyse the results concerning the Intense Observation Periods, including both permanent stations and passive diffusion tubes. Aim of this analysis is to evaluate the accuracy of the model in reproducing the spatial inhomogeneities of the ground level pollutant concentration on the whole domain. As shown in Fig. 4, SIRANE results are in a general good agreement with the weekly averaged concentration measured. Nevertheless, we notice that the larger biases are observed in the locations where the concentrations are the highest.

A rapid overview of the results presented in Fig. 6 suggests that results in the IOP1 and IOP2 show less bias than those in the IOP 3, i.e. that the model performs better in winter/spring rather than in summer. We will further comment on this in the analysis of the results, at the end of sect. 5.

As a second step, we focus on the comparisons between modelled and measured hourly averaged concentrations on these fixed monitoring stations. We begin by focusing on temporal signals registered in four stations, which are representative of the four categories previously identified: suburban (Côtiere de l'Ain), industrial (Feyzin), traffic road (Mulatière) and urban (Lyon centre).

Data referring to the first IOP are presented in Fig. 7 and show that SIRANE reproduces accurately the temporal variations of NO_2 concentrations, even though the gap between the two is sometimes large, exceeding a factor of two. Note in particular the clear discrepancies occurring at the Mulatière station, where the model is unable to reliably predict the peaks of pollution in the early morning, at the rush hour. This feature will be analysed in detail in sect. 5.

Modelling results provided by SIRANE show a high spatial variability of NO_2 concentration over the domain (see the graphical abstract, showing a map of the annual mean concentration for the Lyon agglomeration and city centre), highlighting the high impact of traffic related pollution.

Measured and modelled annual mean concentrations, respectively μ_{Mes} and μ_{SIR}, are generally in good agreement (Fig. 8). Nevertheless, as already noticed in case of weekly averages, the bias can be larger than 10 $\mu g\ m^{-3}$ in correspondence to the stations

Table 2
List of the statistical indices used to quantify the accordance between the numerical and the experimental data sets; C_m and C_p are the measured and predicted concentrations, respectively.

| Index	Definition	Optimal value	Criteria
Fractional bias	$FB = \frac{2(\overline{C_m} - \overline{C_p})}{(\overline{C_m} + \overline{C_p})}$	0	$-0.3 \leq FB \leq 0.3$
Relative error	$ER = \overline{\left(\frac{2|C_m - C_p|}{(C_m + C_p)}\right)}$	0	
Normal mean square error	$NMSE = \frac{\overline{(C_m - C_p)^2}}{\overline{C_m} \, \overline{C_p}}$	0	$\sqrt{NMSE} \leq 2$
Correlation coefficient	$Corr = \frac{\overline{(C_m - \overline{C_m})(C_p - \overline{C_p})}}{\sqrt{\overline{(C_m - \overline{C_m})^2}\,\overline{(C_p - \overline{C_p})^2}}}$	1	
Geometric mean bias	$MG = exp(\overline{ln(C_m)} - \overline{ln(C_p)})$	1	$0.7 \leq MG \leq 1.3$
Geometric variance	$VG = exp(\overline{(ln(C_m) - ln(C_p))^2})$	1	$VG \leq 1.6$
Fraction in a factor of 2	FAC2: fraction of data that satisfy $0.5 \leq \frac{C_p}{C_m} \leq 2$	1	$FAC2 \geq 0.5$
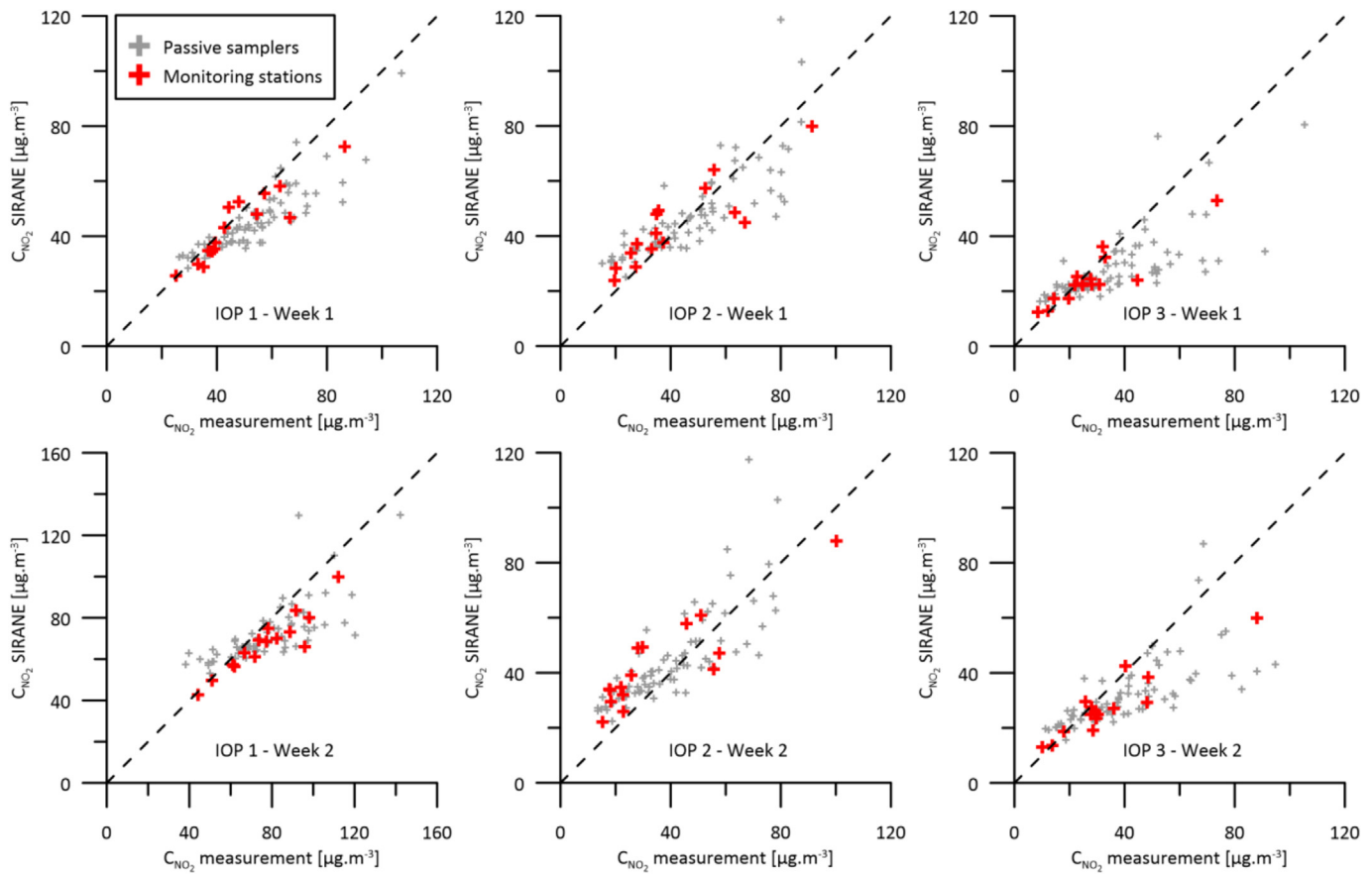
Fig. 6. Comparison of simulated and measured NO_2 mean concentrations for the different Intensive Observational Periods [$\mu g.m^{-3}$].

where the concentration are the highest (larger than 55 $\mu g\ m^{-3}$). The values of the bias are positive (Table 3), implying that concentrations are generally underestimated by the model.

The model performances (Table 3) shows that SIRANE satisfies all criteria suggested by Chang and Hanna (2004) and Chang et al. (2005), for all monitoring stations, except for one, the monitoring station Vaise, where the indices FB (0.38) and MG (1.53) exceed the limits. Something similar also occurs for the station named Mulatière where FB (0.26 and 0.16 respectively) and MG (1.27 and 1.18 respectively) are relatively large, even though they are within the Chang and Hanna (2004) limits.

Results in Table 3 highlights the general tendency of SIRANE in underestimating pollutant concentration, especially for the

monitoring stations placed close to the most congested traffic axes: Grand-Clément, Lyon périphérique, Gerland. Note that these underestimations do not depend on the location of the receptors and concern evenly measurement stations placed within street canyons and in 'open field'. For this reason, the discrepancies between model and measurements cannot be specifically attributed to the parametric laws adopted to simulate pollutant transfer within the urban canopy. A possible explanation for these discrepancies is related to vehicles emissions factors, whose modelled values, as suggested by previous authors (e.g. Berkowicz et al., 2006; Smit et al., 2008), are suspected to underestimate the real ones. Recently, O'Driscoll et al. (2010) provide evidence that COPERT modelling results significantly underestimate NO2 and NOx
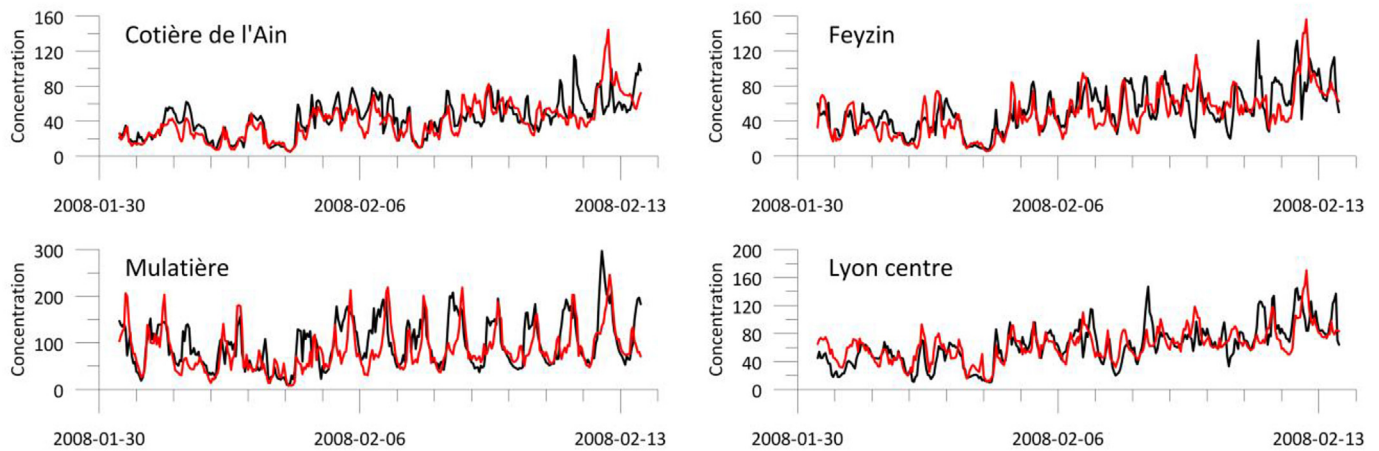
Fig. 7. Comparison of the NO$_2$ concentration during the IOP 1; measurements are in black whereas SIRANE results are in red. (For interpretation of the references to colour in this figure legend, the reader is referred to the web version of this article.)
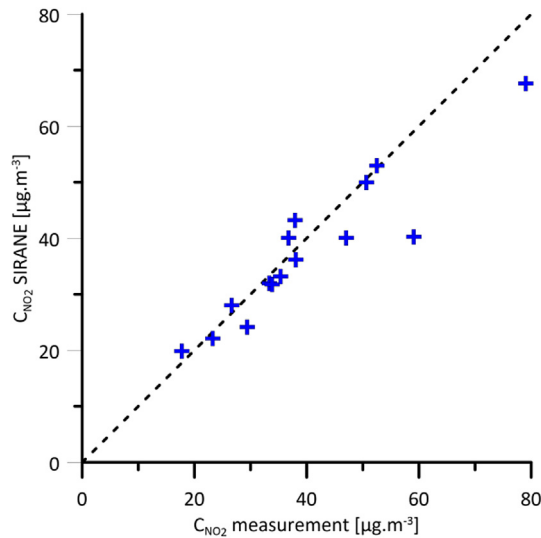
Fig. 8. Comparison between modelled and measured NO$_2$ annual means concentration [μg.m^{-3}] at the 15 permanent monitoring stations.

emission from Euro 6 diesel cars. Jaikumar et al. (2017) show that the standard emission models (like COPERT) under predict the real emissions by 30–200%, depending upon different driving modes. Note however that, based on our results, we are not in the position of proving that this is the actual cause for the underestimations in the model predictions.

5. Discussion

We evaluate the model performances depending on the meteorological input parameters, namely the wind intensity (U), the wind direction (θ) and the stability condition (L_{MO}^{-1}), and the location of the measurements points (street canyons, proximity of roads, etc…). We focus on two statistical indices only, FB and NMSE. Note that this analysis is different from a 'classical' sensitivity analysis, as the one presented in the part II of this study (Soulhac et al., 2012), evaluating the effects of a progressive variation of the values of the input data on the model output.

To that purpose we begin by dividing the 15 stations in five different groups: urban traffic stations (located in street canyons), sub-urban traffic stations (located in 'open field'), urban (located in

Table 3
Comparison of SIRANE results with data from the monitoring stations during 2008 (bold red values exceed the criteria of Chang and Hanna (2004) and Chang et al. (2005)).

	μ$_{Mes}$ [μg.m^{-3}]	μ$_{SIR}$ [μg.m^{-3}]	FB	ER	NMSE	Corr	MG	VG	FAC2
Optimal value			0 0.3 ≤ FB ≤ 0.3	0	0 NMSE^2 ≤ 4	1	1 0.7 ≤ MG ≤ 1.3	1 VG ≤ 1.6	1 FAC2 ≥ 0.5
COT	23.26	22.11	0.05	0.38	0.25	0.79	1.00	1.32	0.83
GEN	33.36	31.95	0.04	0.40	0.23	0.71	0.99	1.38	0.81
STE	17.78	19.81	−0.11	0.28	0.06	0.96	0.81	1.15	0.90
TER	29.41	24.15	0.20	0.47	0.35	0.65	1.20	1.52	0.74
BER	52.50	52.93	−0.01	0.34	0.18	0.64	1.02	1.24	0.87
GC	47.06	40.06	0.16	0.43	0.33	0.65	1.09	1.38	0.79
LP	50.67	49.97	0.01	0.41	0.26	0.63	1.00	1.34	0.81
MUL	79.05	67.59	0.16	0.44	0.31	0.60	1.18	1.41	0.78
VAI	59.10	40.20	**0.38**	0.49	0.38	0.66	**1.53**	1.52	0.73
FEY	33.84	31.72	0.06	0.44	0.30	0.59	1.06	1.46	0.76
STF	35.35	33.14	0.06	0.40	0.30	0.71	0.99	1.34	0.82
GER	38.08	36.13	0.05	0.39	0.25	0.67	1.01	1.31	0.83
LC	37.95	43.18	−0.13	0.41	0.24	0.66	0.83	1.35	0.80
STJ	36.78	40.05	−0.09	0.41	0.26	0.67	0.87	1.35	0.80
VAU	26.67	28.00	−0.05	0.45	0.26	0.75	0.82	1.48	0.77

a dense urban area but away from busy roads), industrial stations (located close to industrial facilities), and background stations (located away from both industrial, residential and traffic sources).

Results of this analysis, presented in Fig. 9, show that the values of FB and of the NMSE exhibit significant variations depending on the values of the meteorological parameters. The indices concerning the traffic stations, both in urban and sub-urban areas, tend to increase for large wind velocities, indicating a degradation of the model estimates. However this tendency cannot be any longer identified in the rest of the urban stations, as well as in the industrial and the background stations. Focusing on the wind direction θ, we observe that the trends of the data relative to the four typologies of stations are very different. This is also what can be observed when analysing the trend of the variations depending on the stability conditions. The global picture is therefore not clear and does not allow us to conclude about an eventual dependence of the model performances on peculiar meteorological conditions. All we can state is that the FB of the traffic stations data (both within the urban area and outside of it) are markedly positive, revealing a general underestimation of the model predictions. The FB of industrial, urban and background stations are instead closer to zero.

To push further our analysis we therefore have to disaggregate our data and analyse the behavior of the data collected station by station. Again, when analyzing the results presented in Fig. 10, we observe that for some stations the performances of the model are clearly worse than for others. However, we cannot clearly identify a unique trend of the evolution of the FB and the NMSE as a function of the values of the meteorological parameters. This means that, in order to explain the discrepancies between model and measurements, we have to analyse singularly the characteristics of each station. In doing so, we restrict our attention to two traffic stations, Vaise and Mulatière, the ones that exhibit the larger discrepancies between measurements and model results.

The worse performances of the results for the Vaise Station can be explained by its location. The district of Vaise is actually bordered by two hills, forming a small valley within which the air circulation is somehow decoupled to that occurring in the rest of the agglomeration. This particular morphological condition can actually produce an accumulation of pollutant within this district, due to the recirculation flows occurring in this small valley. This complex air circulation is not reproduced by the SIRANE meteorological input, which actually assumes that the flow over the whole urban area is modelled according to Monin-Obhukov similarity theory, i.e. homogeneity on the horizontal plane. SIRANE is therefore not able to simulate any of these effects inducing an accumulation of air pollutant within this district. Its predictions tend then to a systematic underestimate of real concentration values. To improve these predictions it would be therefore necessary to include more complex three dimensional meteorological fields over the domain.

Concerning the Mulatière station, there are two main features that deserve to be discussed. The first concerns the bad model performances for wind directions that are close to $\theta = 270°$, the second those occurring for highly unstable conditions, i.e. large negative values of L_{MO}^{-1}. As shown in Fig. 12, when $\theta \approx 270°$, the FB is close to 0.6 and the NMSE attains 0.8. To explain this we refer to Fig. 11a, where we show the details of the location of the measurement station. This is located nearby the highway (direction N-S) and relatively close to a long and tall building. It is worth remembering that SIRANE does not distinguish the case of a street which is partially bordered by buildings from the case of a street in open field (not bordered by building at all). Therefore, according to the model, when the wind direction is $\theta = 270°$ the measurements station will not intercept the pollutant plume generated by the line source representing the traffic emissions along the highway. In the

reality, however, the presence of an elongated building beside the highway produces a recirculating region in its wake. This recirculating flow pattern can then induce for the transport of the pollutant plume in the opposite direction to that of the overlying wind (Fig. 11b). There is therefore a direct contribution of the traffic emissions along the highway on the concentrations registered at the station which is completely neglected by the model. This feature is likely to explain the large values of FB and NMSE, and therefore the significant underestimation of the model predictions, for these peculiar wind directions. This example enlightens the need of introducing new parameterisations in the model for the dispersion in streets that are only partially bordered by buildings.

Concerning the influence of the stability condition, we clearly notice (Fig. 10) that, for unstable conditions ($L_{MO}^{-1} < -0.8$), the model performances are significantly deteriorated. This is the main reason for the systematic discrepancies observed in the time series of the concentrations initially presented in Fig. 7. The time series of NO_2 concentrations registered at the Mulatière station presented in Fig. 7 are also shown in Fig. 12, where we also superpose the evolution of L_{MO}^{-1}. It is evident that in correspondence of negative peak of L_{MO}^{-1}, in the second part of the time series, the model systematically underestimates the concentration, and is unable to reproduce the peak characterising the morning rush hour. The reason for this is likely to rely on the parameterisation of the plume width in case of strongly unstable atmospheric conditions and that over predicts the dispersion and the mixing close to the source. Note that this feature can also provide a reliable explanation for the better performances of the model in simulating pollutant dispersion during the winter and the spring time rather than in summer, as suggested by the scatter plot presented in Fig. 6. The improvement of the near-field dispersion of traffic-related ground-level plumes is therefore an aspect that requires further research work, which in turn will require specific in-situ observations by several measurement stations.

6. Conclusion

This paper presents a validation study of the SIRANE 2.0 urban air quality model, whose performances have been evaluated against on site measurements of nitrogen dioxide over the Lyon urban area and over a whole year. This new version of SIRANE includes algorithms to treat distributed pollutant emissions over a whole urban agglomeration. The model validation was performed by a systematic comparison with NO_2 concentration measurements obtained through three intensive measurement campaigns by means of 75 measurement points equipped by passive diffusion tubes and through continuous measurements of hourly averaged concentrations from 15 permanent monitoring stations (over the whole year 2008). Based on the criteria proposed by Chang and Hanna (2004) and Chang et al. (2005), the overall model performances can be considered as « good », in reproducing both the temporal and spatial variability of NO_2 concentrations. Nevertheless, results clearly show that SIRANE has a tendency in underestimating the experimental values, notably those registered close to the most congested traffic axes. These differences have been discussed and related to the influence of peculiar physical processes. This analysis allowed us to identify three possible modifications to improve the model: i) the inclusion of a three-dimensional velocity field over the urban agglomeration, which would make SIRANE more reliable to simulate dispersion in cities characterised by the presence of a complex orography: ii) the parameterisations of the dispersion in streets partially bordered by buildings, i.e. that cannot be considered as 'street canyons' but in which flow and dispersion are highly affected by the buildings wakes; iii) the parameterisation of the near-field dispersion of
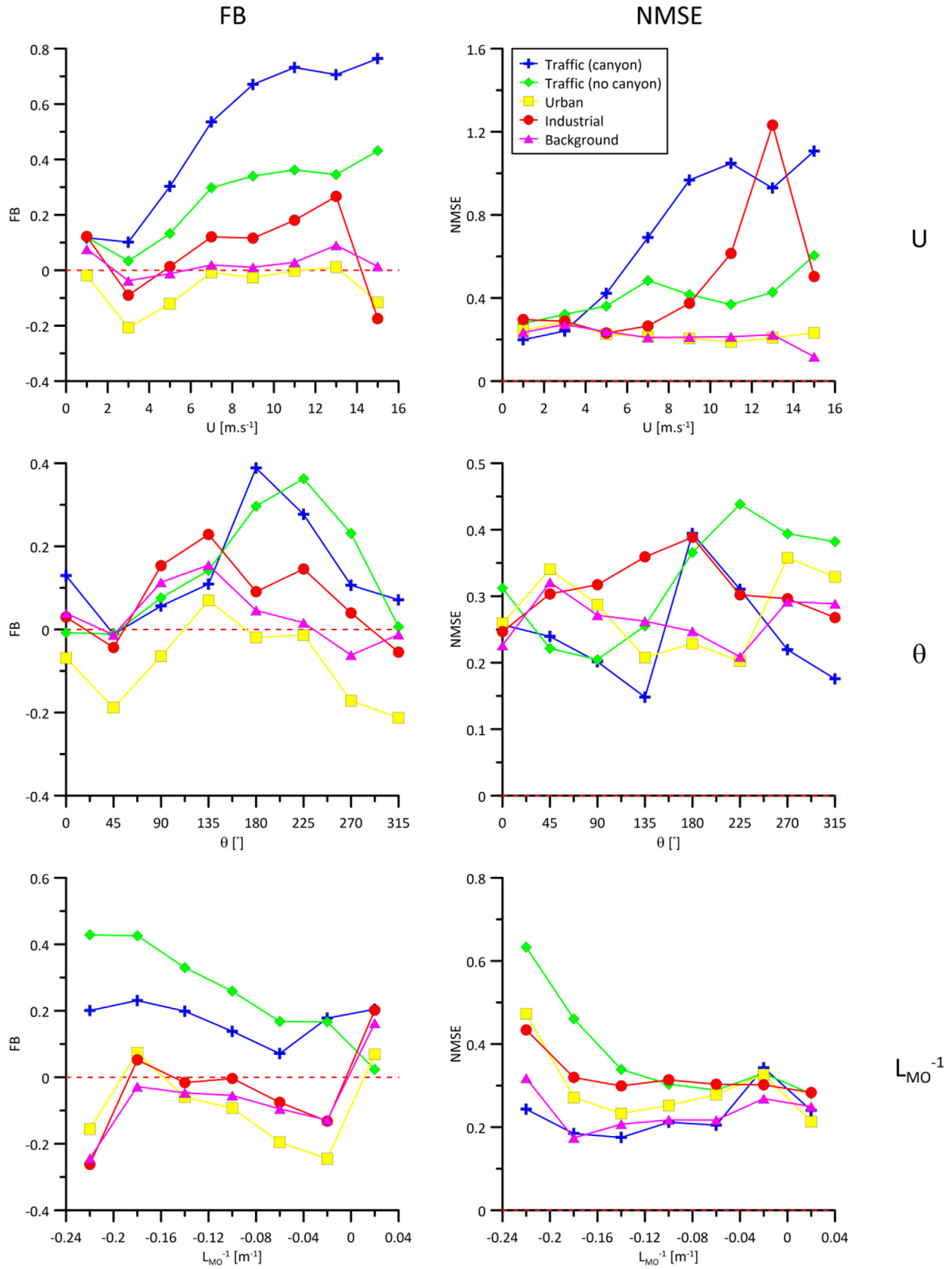
Fig. 9. Evaluation of the FB and NMSE as a function of three meteorological parameters, i.e. wind velocity U, wind direction θ and inverse of the Monin-Obukhov length, for the four typologies of monitoring stations.
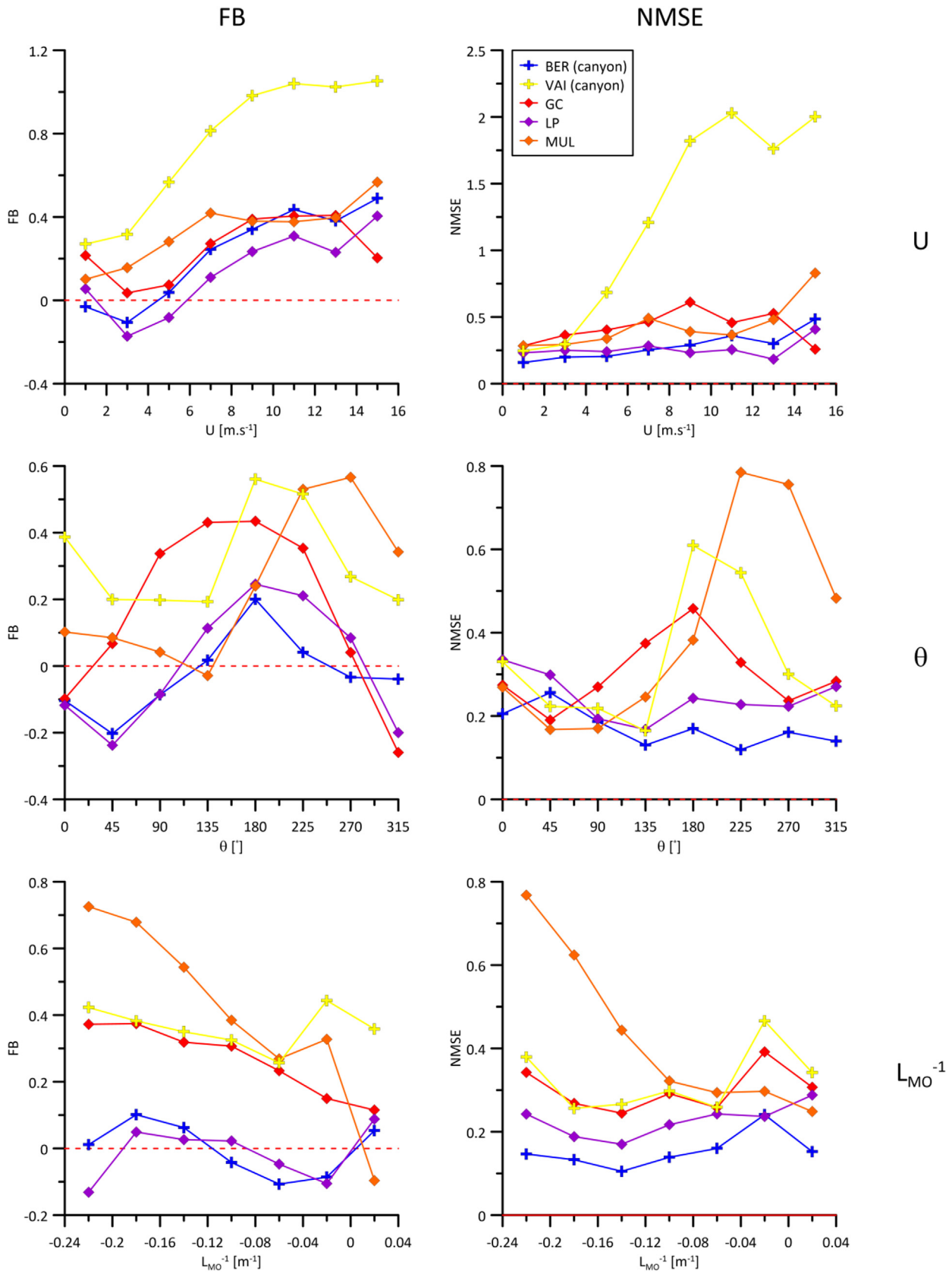
Fig. 10. Evaluation of the FB and NMSE as a function of three meteorological parameters, i.e. wind velocity U, wind direction θ and inverse of the Monin-Obukhov length, for the six monitoring stations referred to as 'traffic' (placed both within street canyons and in open field).

a)

b)
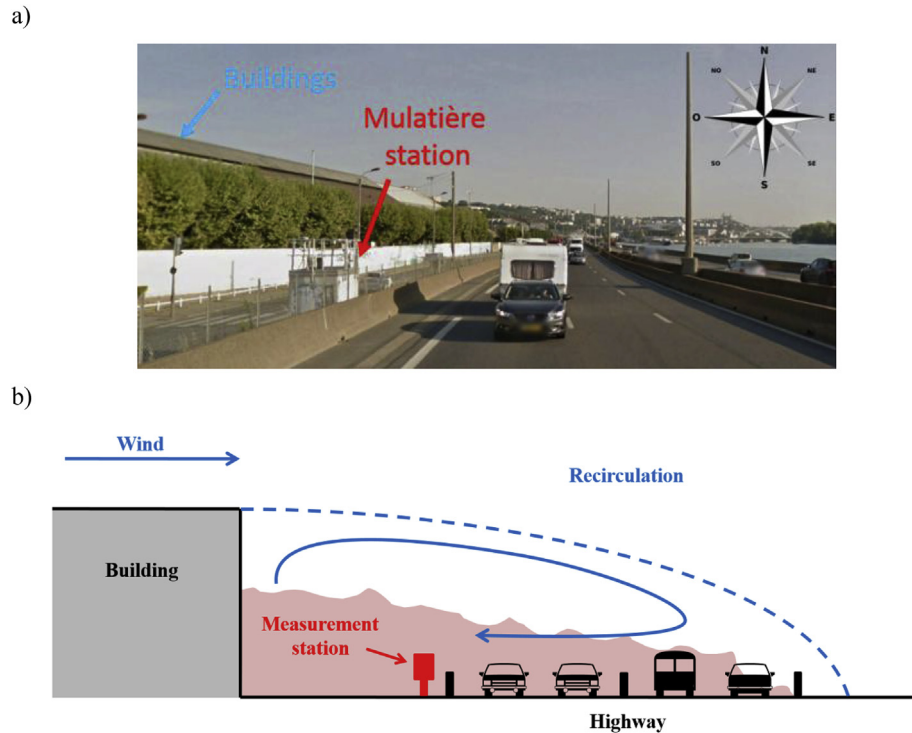
Fig. 11. Mulatière monitoring station: a) photograph of the station, placed beside the highway and close to a long building b) sketch of flow and dispersion patterns in the wake of the long building for a wind direction equal to $\theta = 270°$.
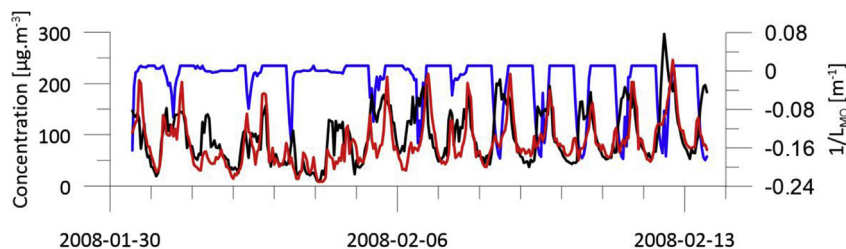
Fig. 12. Measured (black) and modelled (red) concentration at Mulatière superposed with the evolution of the inverse of the Monin-Obhukov length (in blue, with values on the right axis). (For interpretation of the references to colour in this figure legend, the reader is referred to the web version of this article.)

pollutant emitted at ground level by vehicular emissions in strongly unstable atmospheric conditions.

References

Belcher, S.E., Coceal, O., Goulart, E.V., Rudd, A.C., Robins, A.G., 2015. Processes controlling atmospheric dispersion through city centres. J. Fluid Mech. 763, 51–81.

Berkowicz, R., Winther, M., Ketzel, M., 2006. Traffic pollution modelling and emission data. Environ. Model. Softw. 21, 454–460.

Biemmi, S., Gaveglio, R., Salizzoni, P., Boffadossi, M., Casadei, S., Bedogni, M., Garbero, V., Soulhac, L., 2010. Estimate of Atmospheric Boundary Layer Parameters for Pollutant Dispersion Modeling in Urban Areas - 31st NATO/SPS International Technical Meeting on Air Pollution Modelling and its Application.

Brown, M.J., Gowardhan, A.A., Nelson, M.A., Williams, M.D., Pardyjak, E.R., 2013. QUIC transport and dispersion modelling of two releases from the Joint Urban 2003 field experiment. Int. J. Environ. Pollut. 52, 263–287.

Carpentieri, M., Salizzoni, P., Robins, A., Soulhac, L., 2012. Evaluation of a neighbourhood scale, street network dispersion model through comparison with wind tunnel data. Environ. Model Softw. 37, 110–124.

Castagnetti, F.B., Salizzoni, P., Garbero, V., Genon, G., Soulhac, L., 2008. Atmosferic pollution modelling in urban areas at local scale: an example of the application to a neighborhood in Turin. Geoing. Ambient. E Mineraria 124, 63–76.

Chang, J.C., Hanna, S.R., 2004. Air quality model performance evaluation. Meteorol. Atmos. Phys. 87, 167–196.

Chang, J.C., Hanna, S.R., Boybeyi, Z., Franzese, P., 2005. Use of salt lake city urban 2000 field data to evaluate the urban hazard prediction assessment capability (HPAC) dispersion model. J. Appl. Meteorol. 44, 485–501.

Cierco, F.X., Soulhac, L., Méjean, P., Lamaison, G., Salizzoni, P., Armand, P., 2010. SIRANERISK: an operational dispersion model for urban areas incorporating a new method to account for concentration fluctuations. In: 13th International Conference on Harmonisation Within Atmospheric Dispersion Modelling for Regulatory Purposes, Paris, France, 1e4 June.

Dėdelė, A., Miškinytė, A., 2015. The statistical evaluation and comparison of ADMS-Urban model for the prediction of nitrogen dioxide with air quality monitoring network. Environ. Monit. Assess. 187, 578.

De Haan, P., 1999. On the use of density kernels for concentration estimations within particle and puff dispersion models. Atmos. Environ. 33, 2007–2021.

Garbero, V., Salizzoni, P., Soulhac, L., 2010. Experimental study of pollutant dispersion within a network of streets. Bound.-Layer Meteorol. 136, 457–487.

Giambini, P., Salizzoni, P., Soulhac, L., Corti, A., 2010. Air quality modelling system

for traffic scenario analysis in Florence: model validation and identification of critical issues. In: Presented at the HARMO 2010-Proceedings of the 13th International Conference on Harmonisation within Atmospheric Dispersion Modelling for Regulatory Purposes, pp. 195—199.

Hanna, S., Chang, J., 2012. Acceptance criteria for urban dispersion model evaluation. Meteorol. Atmos. Phys. 116, 133—146.

Harsham, K.D., Bennett, M., 2008. A sensitivity study of the validation of three regulatory dispersion models. Am. J. Environ. Sci. 4, 63—76.

Jacquemin, B., Lepeule, J., Boudier, A., Arnould, C., Benmerad, M., Chappaz, C., Ferran, J., Kauffmann, F., Morelli, X., Pin, I., Pison, C., Rios, I., Temam, S., Künzli, N., Slama, R., Siroux, V., 2013. Impact of geocoding methods on associations between long-term exposure to urban air pollution and lung function. Environ. Health Perspect. 121, 1054—1060.

Jaikumar, R., Shiva Nagendra, S.M., Sivanandan, R., 2017. Modal analysis of real-time, real world vehicular exhaust emissions under heterogeneous traffic conditions. Transp. Res. Part D Transp. Environ. 54, 397—409.

Mohan, M., 2011. Performance evaluation of AERMOD and ADMS-urban for total suspended particulate matter concentrations in megacity Delhi. Aerosol Air Qual. Res. http://dx.doi.org/10.4209/aaqr.2011.05.0065.

Morelli, X., Rieux, C., Cyrys, J., Forsberg, B., Slama, R., 2016. Air pollution, health and social deprivation: a fine-scale risk assessment. Environ. Res. 147, 59—70.

Nash, D.G., Leith, D., 2010. Use of passive diffusion tubes to monitor air pollutants. J. Air Waste Manag. Assoc. 60, 204—209.

Ntziachristos, L., Samaras, Z., 2000. COPERT III Computer Programme to Calculate Emissions from Road Transport: Methodology and Emission Factors (Tech. Rep. No. 49). Cph. Den. Eur. Environ. Agency. Retrieved March 21, 2006, Version 2.1. .

O'Driscoll, R., ApSimon, H.M., Oxley, T., Molden, N., Stettler, M.E.J., Thiyagarajah, A., 2010. A Portable Emissions Measurement System (PEMS) study of NOx and primary NO2 emissions from Euro 6 diesel passenger cars and comparison with COPERT emission factors. Atmos. Environ. 145, 8191.

Ouidir, M., Giorgis-Allemand, L., Lyon-Caen, S., Morelli, X., Cracowski, C., Pontet, S., Pin, I., Lepeule, J., Siroux, V., Slama, R., 2015. Estimation of exposure to atmospheric pollutants during pregnancy integrating space—time activity and indoor air levels: does it make a difference? Environ. Int. 84, 161—173. http://dx.doi.org/10.1016/j.envint.2015.07.021.

Padilla, C.M., Kihal-Talantikit, W., Vieira, V.M., Deguen, S., 2016. City-specific spatiotemporal infant and neonatal mortality clusters: links with socioeconomic and air pollution spatial patterns in France. Int. J. Environ. Res. Public. Health 13, 624.

Pineda Rojas, A.L., Venegas, L.E., 2013. Upgrade of the DAUMOD atmospheric dispersion model to estimate urban background NO2 concentrations. Atmos. Res. 120—121, 147—154. http://dx.doi.org/10.1016/j.atmosres.2012.08.010.

Pouliot, G., Denier van der Gon, H.A.C., Kuenen, J., Zhang, J., Moran, M.D., Makar, P.A., 2015. Analysis of the emission inventories and model-ready emission datasets of Europe and North America for phase 2 of the AQMEII project. Atmos. Environ. 115, 345—360.

Righi, S., Lucialli, P., Pollini, E., 2009. Statistical and diagnostic evaluation of the ADMS-Urban model compared with an urban air quality monitoring network. Atmos. Environ. 43, 3850—3857.

Salem, N.B., Garbero, V., Salizzoni, P., Lamaison, G., Soulhac, L., 2015. Modelling pollutant dispersion in a street network. Bound.-Layer Meteorol. 155, 157—187. http://dx.doi.org/10.1007/s10546-014-9990-7.

Seinfeld, J.H., 1986. Atmospheric Chemistry and Physics of Air Pollution, 1 edition. Wiley-Interscience, New York.

Silver, J.D., Brandt, J., Hvidberg, M., Frydendall, J., Christensen, J.H., 2013. Assimilation of OMI NO2 retrievals into the limited-area chemistry-transport model DEHM (V2009.0) with a 3-D OI algorithm. Geosci. Model Dev. 6, 1—16.

Smit, R., Poelman, M., Schrijver, J., 2008. Improved road traffic emission inventories by adding mean speed distributions. Atmos. Environ. 42 (2008), 916—926.

Soulhac, L., 2000. Modélisation de la dispersion atmosphérique à l'intérieur de la canopée urbaine. PhD thesis. École Centrale de Lyon, p. 345.

Soulhac, L., Puel, C., Duclaux, O., Perkins, R.J., 2003. Simulations of atmospheric pollution in Greater Lyon an example of the use of nested models. Atmos. Environ. 37, 5147—5156. http://dx.doi.org/10.1016/j.atmosenv.2003.03.002.

Soulhac, L., Salizzoni, P., Cierco, F.-X., Perkins, R., 2011. The model SIRANE for atmospheric urban pollutant dispersion; part I, presentation of the model. Atmos. Environ. 45, 7379—7395.

Soulhac, L., Salizzoni, P., Mejean, P., Didier, D., Rios, I., 2012. The model SIRANE for atmospheric urban pollutant dispersion; PART II, validation of the model on a real case study. Atmos. Environ. 49, 320—337.

Stocker, J., Hood, C., Carruthers, D., McHugh, C., 2012. ADMS-Urban: developments in modelling dispersion from the city scale to the local scale. Int. J. Environ. Pollut. 50, 308—316.

Tchepel, O., Costa, A.M., Martins, H., Ferreira, J., Monteiro, A., Miranda, A.I., Borrego, C., 2010. Determination of background concentrations for air quality models using spectral analysis and filtering of monitoring data. Atmos. Environ. 44, 106—114.

Tinarelli, G., Mortarini, L., Castelli, S.T., Carlino, G., Moussafir, J., Olry, C., Armand, P., Anfossi, D., 2012. Review and validation of MicroSpray, a lagrangian particle model of turbulent dispersion. Geophys. Monogr. Ser. 200, 311—327.